Terminal Velocity and Shape of Cloud and Precipitation Drops Aloft

K. V. BEARD[1]

Department of Meteorology, University of California, Los Angeles

(Manuscript received 11 November 1975, in revised form 3 February 1976)

ABSTRACT

The terminal velocity of cloud and precipitation size drops has been analyzed for three physically distinct flow regimes: 1) slip flow about a water drop treated as rigid sphere at negligible Reynolds numbers, 2) continuum flow past a water drop treated as a rigid sphere with a steady wake at low and intermediate Reynolds numbers, and 3) continuum flow around a non-circulating water drop of equilibrium shape with an unsteady wake at moderate to large Reynolds numbers. In the lower regime the effect of slip was given by the first-order Knudsen number correction to Stokes drag. In the middle regime a semiempirical drag relation for a rigid sphere was used to obtain a formula for the Reynolds number in terms of the Davies number. In the upper regime a correlation of wind tunnel measurements on falling drops was used in conjunction with sea level terminal velocities for raindrops to obtain a formula for the Reynolds number in terms of the Bond number and physical property number.

The result for the upper regime gave values of the drag coefficient that were consistent with an invariance of shape with altitude in the atmosphere. Simple formulas are given for obtaining the axis ratio and projected diameter as a function of the equivalent spherical diameter. The resulting formulas for the terminal velocity in three diameter ranges (0.5 μm–19 μm, 19 μm–1.07 mm, 1.07 mm–7 mm) may be used to calculate the terminal velocity directly from the equivalent spherical diameter and the physical properties of the drop and atmosphere.

1. Introduction

An accurate knowledge of the terminal velocity and shape of cloud and precipitation drops is needed for carrying out computations in cloud physics as well as for interpreting Doppler radar data. Among others, Laws (1941), Gunn and Kinzer (1949) and Beard and Pruppacher (1969) have measured the terminal velocity of drops for laboratory conditions at sea level whereas the shape of falling drops at sea level has been determined, for example, by Jones (1959), Pruppacher and Beard (1970) and Pruppacher and Pitter (1971). Even though little if any reliable data are available at other atmospheric conditions, it is within the scope of our present knowledge to derive reasonably accurate values for the terminal velocity of water drops for conditions typical in the atmosphere. Since no unified treatment of this problem exists and several erroneous treatments are found in the current literature, the author has been motivated to evaluate the available theoretical and empirical information on drops falling in gases in order to derive a reliable method for obtaining the terminal velocity and shape of a water drop at any level in the atmosphere.

2. Theoretical basis

The complete physical-mathematical basis for the terminal velocity and shape of a falling drop is given by the Navier-Stokes equations of motion for the air flowing past the drop as well as the motion of the water inside the drop subject to the appropriate dynamic and kinematic boundary conditions.[2] Only the steady-state form of these equations at low and intermediate Reynolds numbers can be handled with present techniques. For example, the drag on a liquid sphere for steady, axisymmetric flow was determined analytically by Rybczynski (1911) and Hadamard (1911) for creeping flow, and numerically by LeClair *et al.* (1972) for low and intermediate Reynolds numbers. An analytic solution for a drop of small deformation was obtained by Taylor and Acrivos (1964) using the singular perturbation technique for steady, axisymmetric flow at low Reynolds numbers. If the terminal velocity and shape are to be determined at moderate to large Reynolds numbers, the theoretical treatment must be considerably simplified. On the other hand, for very small cloud droplets there arises a problem in the application of the Navier-Stokes equations because the assumption of a continuous surrounding fluid no longer holds near the droplet surface.

In order to undertake the terminal velocity and shape problem, it is helpful to employ the reasoning of dimensional analysis using Rayleigh's method or the Buckingham Pi Theorem. This permits the reduction of the number of variables to the essential dimensionless groups (e.g., see Perry and Chilton, 1973). The

[1] Present Affiliation: Laboratory for Atmospheric Research, University of Illinois, and Illinois State Water Survey, Urbana 61801.

[2] An extensive treatment of the theory at low Reynolds number may be found in Happle and Brenner (1965).

variables for a liquid drop falling in still air are related by an equation in the form

$$f(t,d_0,V,\rho,\eta,\eta_i,\sigma,D)=0, \quad (1)$$

where the diameter (d_0), the velocity (V), and air density (ρ) may be used in Rayleigh's method to form five independent dimensionless groups: the Reynolds number (N_{Re}), the viscosity ratio (η/η_i), the drag coefficient (C_D), the Bond number (N_{Bo}) and the Strouhal number (N_{Sr}).[3] Obviously, some simplifying assumptions must be made based on sound theoretical or empirical knowledge in order to obtain an adequate description of the coupled terminal velocity and drop shape problem. In the above analysis the Reynolds number is undoubtedly a key dimensionless group. In the subsequent discussion of the terminal velocity and shape of cloud drops and raindrops the problem will be divided into drop size ranges that correspond to three Reynolds number regimes for steady, free stream flow:

Regime 1: small cloud droplets, $1\ \mu\mathrm{m}\lesssim d_0\lesssim 20\ \mu\mathrm{m}$ (*steady wake*, vanishingly small Reynolds numbers, $10^{-6}\lesssim N_{\mathrm{Re}}\lesssim 0.01$).

Regime 2: large cloud droplets to small raindrops, $20\ \mu\mathrm{m}\lesssim d_0\lesssim 1$ mm (*steady wake*, low to intermediate Reynolds numbers, $0.01\lesssim N_{\mathrm{Re}}\lesssim 300$).

Regime 3: small to large raindrops, $1\ \mathrm{mm}\lesssim d_0\lesssim 7$ mm (*unsteady wake*, moderate to large Reynolds numbers, $300\lesssim N_{\mathrm{Re}}\lesssim 4000$).

3. Small cloud droplets ($1\ \mu\mathrm{m}\lesssim d_0\lesssim 20\ \mu\mathrm{m}$)

For such tiny airborne particles the terminal velocity is so small ($V_\infty\lesssim 1$ cm s^{-1}) that it may be considered negligible for many meteorological purposes. On the other hand, reliable values of the differential settling velocity of droplet pairs are needed for computing collision efficiencies. Also, accurate values of the terminal velocity are important for determining the droplet size in laboratory experiments. Since the Stokes terminal velocity of a 1 μm water droplet is in error by as much as 17%, it is worthwhile to consider methods that permit greater accuracy.

In the range of droplet sizes the ratio of the mean free path (l) of air molecules to the droplet diameter lies between 0.003 and 0.07. Thus, the Knudsen number ($N_{\mathrm{Kn}}=l/d_0$) is small but not negligible and the air flow is in a regime between transitional and continuum flow. The drag on a rigid sphere in this near-continuum region has been determined from hydrodynamic theory for slip flow (Bassett, 1961), from kinetic theory (Epstein, 1924), and from experiments (Knudsen and Weber, 1911), all resulting in similar first-order corrections to Stokes drag:

$$D=D_s(1-cN_{\mathrm{Kn}}), \quad (2)$$

where $D_s=3\pi\eta d_0V$. Unfortunately, the proportionality constant (c) is not attainable from hydrodynamic theory so the actual value of c and the higher order Knudsen number corrections must be obtained empirically. Davies (1945) examined the early experimental results of Knudsen and others, and determined the best coefficients in the slip correction factor given in the expression

$$C_{sc}=1+(2l/d_0)[1.257+0.400\exp(-1.10d_0/2l)]=1+c'N_{\mathrm{Kn}}, \quad (3)$$

where $C_{sc}\equiv D_s/D$. The proportionality constant in (2) is seen to be equivalent to c' for small Knudsen numbers. The above empirical correction to Stokes drag should be used with Davies' value for the mean free path at 1 atm obtained by comparing his Eqs. (9) and (10) [i.e., $l_0=6.62\times10^{-6}$ cm]. His formula for the pressure dependence of the mean free path ($l=7.16\times10^{-4}/p$ with p in cm Hg) should not be used since l_0 determined in this manner is 9.42×10^{-6} cm. On the other hand, one may obtain the free path directly from the definition of viscosity given by kinetic theory in Chapman and Cowling (1970) with the mean molecular speed evaluated in terms of the pressure and density. The resulting expression is

$$l=(\eta/0.998)(\pi/2\rho p)^{\frac{1}{2}}, \quad (4)$$

which yields $l_0=6.54\times10^{-6}$ cm using the currently accepted value of $\eta=1.818\times10^{-4}$ g cm^{-1} s^{-1} at 20°C. The pressure dependence of the mean free path is then $l=4.97\times10^{-4}/p_0$, with p in cm Hg. Thus Davies expression appears to be in error by a factor of $\sim2^{\frac{1}{2}}$.

There is no point in adjusting the coefficients in Davies' formula to the modern value of l_0 since this would not effect C_{sc} determined by (3). The use of (3), then, requires $l_0=6.62\times10^{-6}$ cm which may be adjusted for different pressures and temperature using

$$l=l_0(\eta/\eta_0)(p_0/p)(T/T_0)^{\frac{1}{2}}, \quad (5)$$

where $\eta_0=1.818\times10^{-4}$ g cm^{-1} s^{-1}, $p_0=1013.25$ mb, $T_0=293.15$ K. This formula differs from those used by Berry and Pranger (1974) and Davies because the present formula accounts for temperature variations. Although the formulas given by (3) and (5) are believed to be the best available, use of most older expressions will not cause significant differences in the terminal velocity of cloud droplets.

The terminal velocity may then be found from the product of the Stokes terminal velocity for a rigid sphere and the slip correction factor:

$$V_\infty=C_{sc}V_{\infty s}=C_{sc}(\Delta\rho g/18\eta)d_0^2, \quad (6)$$

where $\Delta\rho=\rho_i-\rho$. The correction factor C_{sc} has a value of 1.01 for $d_0=20\ \mu$m and increases to 1.17 for $d_0=1\ \mu$m. Since at $d_0=0.5\ \mu$m the exponential term in (3) has risen to only 0.002, it is not necessary to use the full expression. For $0.5\leqslant d_0\leqslant 20\ \mu$m the first-order Knudsen

[3] A list of symbols is found in the Appendix.

term will suffice. This simplifies Eq. (3) to

$$C_{sc}=1+2.51l/d_0 \tag{7}$$

so that (6) then reduces to the well-known Stokes-Cunningham equation. The essential formulas for computing terminal velocities of small cloud droplets are summarized in Table 1 (part 1).

4. Large cloud droplets and small raindrops ($20\ \mu m \lesssim d_0 \lesssim 1$ mm)

a. Observed flow regimes

In the last section the experimentally determined drag on a droplet at very low Reynolds numbers in the transition flow region was found to be predictable from the drag on a *rigid sphere*. In this section the rigid sphere approximation is examined for water drops as large as 1 mm diameter.

The observed flow regimes about a rigid sphere for a continuous fluid ($N_{Kn} \ll 1$) are compiled in Fig. 1 from the works of Möller (1938), Taneda (1956), Magarvey and MacLatchy (1965) and Achenbach (1974). The flow is seen to progress through a series of transitions from a laminar, symmetrical flow at $N_{Re}=0$ to a separated, turbulent boundary layer flow with a chaotic wake for $N_{Re} \gtrsim 400{,}000$. The flow is apparently quite steady for $N_{Re} \lesssim 300$ although it is no longer axisymmetric above $N_{Re} \approx 200$ because of the formation of twin vortex trails. The steady transversal motion of a falling drop observed by Gunn (1949) is believed by Magarvey and MacLatchy to be the result of a net sideward force due to wake asymmetry in this flow regime.[4] The steady-flow regime ($N_{Re} \lesssim 300$) corresponds to raindrops with $d_0 \lesssim 1$ mm based on the observed Reynolds number for falling water drops (Gunn and Kinzer, 1949). Consequently, it is to be expected for $d_0 \lesssim 1$ mm that the significant variables which characterize the terminal velocity problem are related by an equation of the form

$$f(d_0, V_\infty, \rho, \eta, \eta_i, \sigma, D)=0. \tag{8}$$

Instead of five independent dimensionless groups, there are now only four (e.g., N_{Re}, C_D, N_{Bo} and η/η_i, where the Bond number $N_{Bo}=\Delta\rho g d_0^2/\sigma$). Since dimensional analysis only provides the method for finding the number of independent variables, it is important to conduct further analysis in order to determine the relative importance of each group.

b. Surface tension effect

The surface tension enters into the problem through the equation for the shape given by LaPlace's formula

[4] The onset of sideward motion has been repeatedly observed by the present author to occur at $N_{Re} \approx 200$ ($d_0 \approx 0.9$ mm) in experiments with drops grown by collision coalescence from cloud droplets in the UCLA cloud tunnel.

TABLE 1. Formulas for calculating the terminal velocity of cloud drops and raindrops in 3 size ranges.

1. $0.5\ \mu m \leqslant d_0 \leqslant 19\ \mu m$

$V_\infty = C_1 C_{sc} d_0^2$

$C_1=\Delta\rho g/(18\eta)$, $C_{sc}=1+2.51l/d_0$

$l=l_0(\eta/\eta_0)(p_0/p)(T/T_0)^{\frac{1}{2}}$

$l_0=6.62\times10^{-6}$ cm, $p_0=1013.25$ mb

$\eta_0=0.0001818$ g cm^{-1} s^{-1}, $T_0=293.15$ K

2. $19\ \mu m \leqslant d_0 \leqslant 1.07$ mm

$V_\infty=\eta N_{Re}/(\rho d_0)$

$N_{Re}=C_{sc}\exp(Y)$

$Y=b_0+b_1X+\cdots+b_6X^6$

$b_0=-0.318657$E$+1$

$\cdot\ =+0.992696$

$\cdot\ =-0.153193$E-2

$\cdot\ =-0.987059$E-3

$\cdot\ =-0.578878$E-3

$\cdot\ =+0.855176$E-4

$b_6=-0.327815$E-5

$X=\log_e(N_{Da})$

$N_{Da}=C_2 d_0^3$

$C_2=4\rho\Delta\rho g/(3\eta^2)$

3. $1.07\ \text{mm} \leqslant d_0 \leqslant 7$ mm

$V_\infty=\eta N_{Re}/(\rho d_0)$

$N_{Re}=N_P^{1/6}\exp(Y)$

$N_P=\sigma^3\rho^2/(\eta^4\Delta\rho g)$

$Y=b_0+b_1X+\cdots b_5X^5$

$b_0=-0.500015$E$+1$

$\cdot\ =+0.523778$E$+1$

$\cdot\ =-0.204914$E$+1$

$\cdot\ =+0.475294$

$\cdot\ =-0.542819$E-1

$b_5=+0.238449$E-2

$X=\log_e(\text{Bo}N_P^{1/6})$

$\text{Bo}=C_3 d_0^2$

$C_3=4\Delta\rho g/3\sigma$

for the mechanical equilibrium of an interfacial surface:

$$\sigma\left(\frac{1}{R_1}+\frac{1}{R_2}\right)=\Delta\mathcal{P}, \tag{9}$$

where R_1 and R_2 are the principal radii of curvature of the interface and $\Delta\mathcal{P}$ is the total pressure differential across the interface. The above equation may be expressed for the curvature at the drop's equator by writing $\Delta\mathcal{P}$ as the sum of the spherical curvature pressure $4\sigma/d_0$, the hydraulic head $\Delta\rho g d_0/2$, and the differential dynamic pressure $p_i'-p'$:

$$\sigma\left(\frac{1}{R_1}+\frac{1}{R_2}\right)=\frac{4\sigma}{d_0}+\frac{\Delta\rho g d_0}{2}+p_i'-p'. \tag{10}$$

From the above equation it can be seen that as long as the spherical pressure $4\sigma/d_0$ is dominant, a variation in surface tension is unimportant.

Water drops falling at terminal velocity are nearly spherical as long as their size is not too large. The observations of Pruppacher and Beard (1970) show that the axis ratio (AR) of falling water drops varied from AR $\approx$ 0.97 at $d_0=1$ mm to AR ≈ 1.00 for $d \lesssim 0.3$ mm. Alternatively, Eq. (10) may be evaluated semi-empirically from the data of LeClair *et al.* (1972). At $d_0=1$ mm such an evaluation shows that the hydraulic and dynamic pressure terms are only a few percent of the spherical pressure term. Consequently, drops with diameters <1 mm are essentially spherical and the surface tension is not a significant variable. The number of variables for the dimensional analysis is reduced by

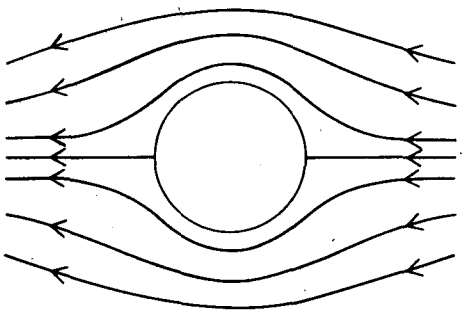

a. Stokes ($N_{Re}=0$). Laminar, steady flow. Streamlines show axial and fore-aft symmetry

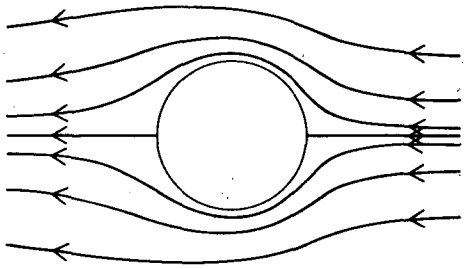

b. Low Reynolds numbers ($0<N_{Re}\lesssim 20$). Laminar, steady axisymmetric flow. Flow no longer has fore-aft symmetry.

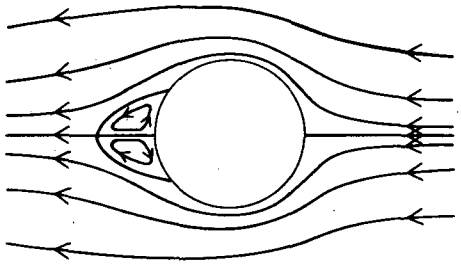

c. Intermediate Reynolds numbers ($20\lesssim N_{Re}\lesssim 200$). Laminar, steady axisymmetric flow, separated with enclosed vortex ring.

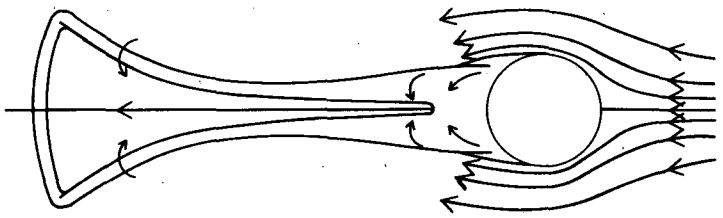

d. Moderate Reynolds numbers ($300\lesssim N_{Re}\lesssim 450$). Vortex loops are formed by roll-up and partial detachment of wake vortex ring. For $200\lesssim N_{Re}\lesssim 300$ steady twin vortex trails are caused by a single loop being carried downstream. Lack of axisymmetry results in steady sideward motion. For $300\lesssim N_{Re}\lesssim 450$ vortex loops detach periodically from diametrical opposite sides of wake axis producing zig-zag motion.*

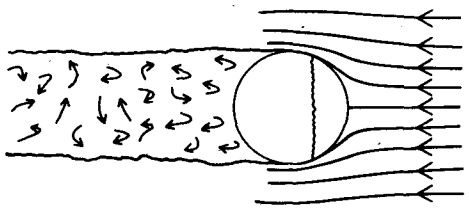

e. Large Reynolds numbers ($N_{Re}\gtrsim 450$). Wake becomes increasingly chaotic at larger Reynolds numbers. Flow separation point moves forward until $N_{Re}\gtrsim 400{,}000$, then abruptly backward with the onset of turbulent boundary layer.*

* Exact nature of wake instabilities and actual values of transition Reynolds numbers are subject to free stream turbulence and boundary effects.

FIG. 1. Flow regimes about a rigid sphere in a laminar, steady, free-stream velocity.

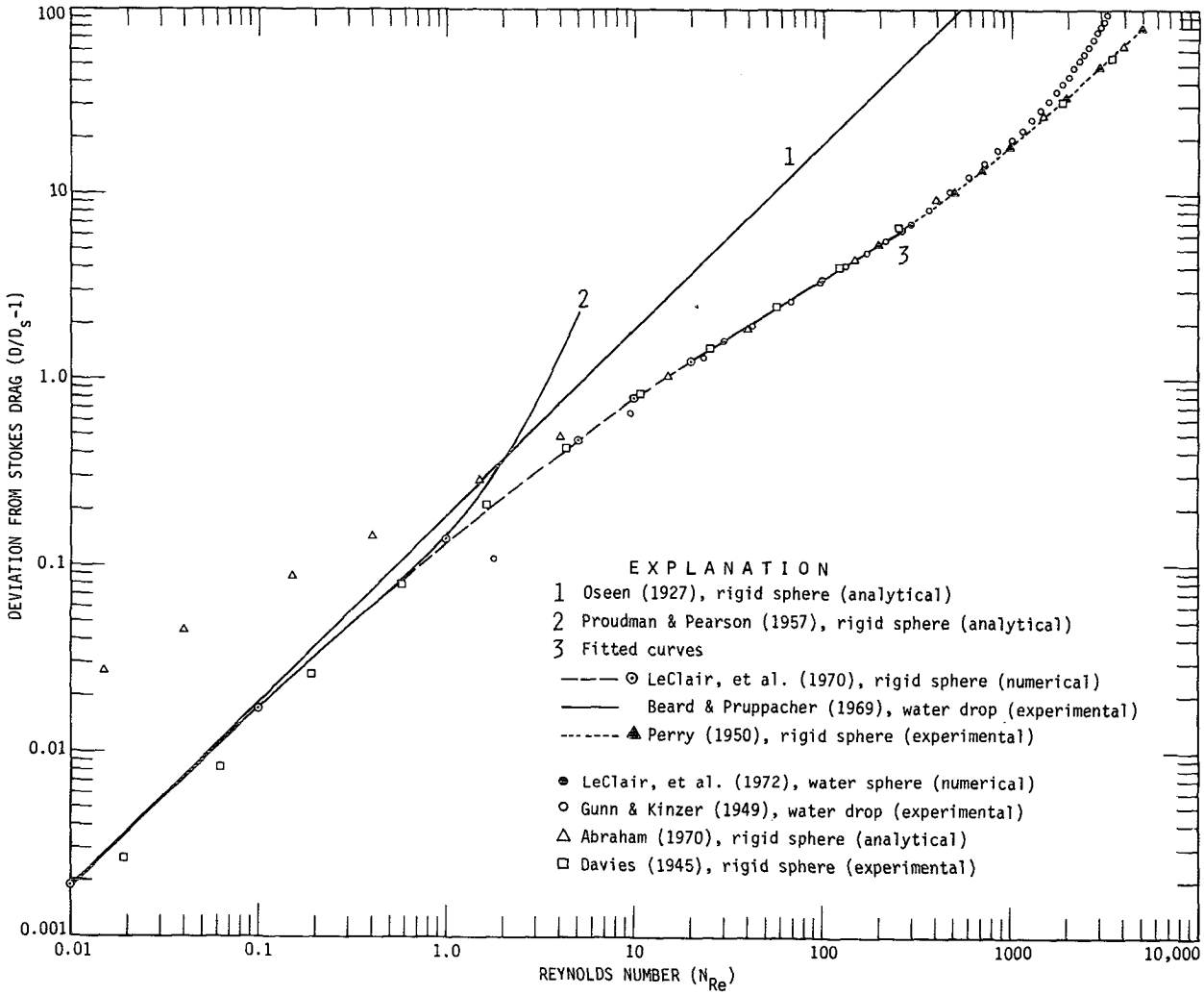

FIG. 2. Deviation of the drag on rigid and liquid spheres and on a water drops falling at terminal velocity from the Stokes drag on a rigid sphere as a function of the Reynolds number.

eliminating σ from (8) which results in only three dimensionless groups (e.g., N_{Re}, C_D, η/η_i).

c. Viscosity ratio effect

The value of the viscosity ratio may be utilized to distinguish between the liquid and rigid sphere problem for it is obvious that as $\eta/\eta_i \to 0$ the drag becomes equivalent to a rigid sphere. However, in order to determine the relative effect of the viscosity ratio in this particular problem, the theoretical and experimental results must be considered for the drag on liquid and rigid spheres.

The flow field inside and outside a liquid sphere was solved analytically by both Hadamard and Rybczynski for vanishingly small Reynolds numbers. Their solution for the magnitude of the drag force in terms of the Stokes drag on a rigid sphere is

$$D = D_s(1-\eta/3\eta_i), \tag{11}$$

where the correction term is seen to be proportional to the viscosity ratio. Consequently, the assumption of a rigid sphere is quite good for very small Reynolds numbers as long as $\eta/\eta_i \ll 1$. Since $\eta/\eta_i \sim 0.018$ for water droplets in air, no distinction was made in the preceding section between the motion of droplets and solid spheres.

d. Drag on rigid and liquid spheres

At larger Reynolds numbers where the Stokes solution no longer applies one may use the results plotted in Fig. 2 to evaluate the drag on rigid and liquid spheres and on water drops falling in air. In this figure the nondimensional variables, N_{Re} and D/D_s-1, are plotted in a manner devised by Maxworthy (1965). At low Reynolds numbers the value of D/D_s-1 is particularly sensitive to deviations from Stokes drag, whereas at higher Reynolds numbers where $D/D_s \gg 1$, this function becomes another form of the drag coefficient since

TABLE 2. Basic drag formulas for the rigid sphere.

$$D/D_s - 1 = \exp(a_0 + a_1 X + a_2 X^2)$$
$$X = \log_e(N_{Re})$$

Range	a_0	a_1	a_2	Data source
$0.01 \leqslant N_{Re} \leqslant 20$	−2.029	+0.8222	−0.02253	LeClair *et al.* (1970)
$20 \leqslant N_{Re} \leqslant 258$	−1.666	+0.6320	0	Beard and Pruppacher (1969)
$258 \leqslant N_{Re} \leqslant 5000$	−0.9100	+0.2619	+0.04214	Perry (1950)

$D/D_s = C_D N_{Re}/24$. The drag at low Reynolds number is seen to deviate from the Stokes drag via the well-known Oseen inertial correction (curve 1). This behavior results from the fact that the Oseen rather than the Stokes solution is the valid zeroth approximation to the Navier-Stokes equation at small Reynolds numbers. A subtle but important change in the drag is noticeable near $N_{Re} = 0.05$ where the deviation proceeds via the inertial correction of Proudman and Pearson (1957) [curve 2]. This is nicely verified by the numerical solutions to the Navier-Stokes equation of LeClair *et al.* (1970). Above $N_{Re} \approx 0.5$ the analytic, low Reynolds number solutions are known to get progressively worse (Pruppacher *et al.*, 1970). However, for $N_{Re} \gtrsim 10$, the simple boundary layer estimate of Abraham (1970) gives a surprisingly good representation of the drag.

It is important to note the measured values of Gunn and Kinzer (1949) for water drops falling in still air. Although their result for the smallest drops are apparently in error due to evaporation [see discussion in Beard and Pruppacher (1969, p. 1071)], their measurements in the range $100 \lesssim N_{Re} \lesssim 400$ correspond closely to the empirical curve of Beard and Pruppacher, the rigid sphere curve of Abraham, and the empirical curve based on Perry (1950). Above $N_{Re} \approx 400$ the drag on a water drop is seen to increase faster than for a solid sphere mainly because of deformation. Some of the difference between the two curves is due to the use of d_0 in calculating the Reynolds number. At $d_0 = 5$ mm the projected diameter is some 11% larger than d_0 (given later in Fig. 4). However, the increase in Reynolds number in going from the drop curve to the sphere curve in Fig. 2 (for $d_0 = 5$ mm) is about 70%. Thus, the difference in the two curves is not just artificial but is mainly due to the intrinsically different flow about deformable drops compared to rigid spheres.

It is quite apparent from Fig. 2 that the drag on a water drop may be closely approximated by the drag on a rigid sphere up to $N_{Re} = 300$. Of course this outcome is expected for $d_0 \lesssim 1$ mm since the surface tension and internal viscosity are known to be insignificant variables (i.e., the drag is unaffected by modest changes in σ and η_i). Shown in Table 2 are the basic drag formulas for the rigid sphere obtained by least-squares fit to the following data. For $0.01 \leqslant N_{Re} \leqslant 20$ the numerical data of LeClair *et al.* (1970) were used to obtain a second-order log-log curve that fits smoothly into the empirical curve of Beard and Pruppacher for $20 \leqslant N_{Re} \leqslant 258$. Above the midrange a second-order log-log curve was fitted to the data of Perry.

e. *Terminal velocity results*

Unfortunately, the formulas in Table 2 are not in a convenient form for computing the terminal velocity from the diameter. The most suitable arrangement of nondimensional groups was devised by Davies (1945) who combined the drag coefficient with the square of the Reynolds number in order to eliminate the terminal velocity:

$$C_D N_{Re}^2 = 4\rho\Delta\rho g d_0^3/(3\eta^2). \tag{12}$$

The velocity may then be obtained from a knowledge of the unique curve for $C_D N_{Re}^2$ vs N_{Re} by first evaluating $C_D N_{Re}^2$ and then V_∞ from the corresponding Reynolds number. This dimensionless group, apparently originated by Davies, is distinct from any other group [e.g., see the listing in the *Handbook of Chemistry and Physics* (CRC, 1973–74 ed.)]. Such a distinct and convenient dimensionless number deserves a name, so it will be referred to as the Davies number ($N_{Da} = C_D N_{Re}^2$) after its originator.

The Davies number was generated from the three basic formulas in Table 2, providing 20 points which were in turn fitted by the least-squares method to obtain a sixth-order polynomial in $X = \log_e(N_{Da})$ and $Y = \log_e(N_{Re})$. The results of this fit are given in Table 1 (part 2) in terms of formulas for computing the terminal velocity of water drops falling in air for various atmospheric conditions in the size range $19\ \mu m \leqslant d_0 \leqslant 1.07$ mm. In order for this midrange to merge smoothly with the lowest range it was necessary to incorporate the slip correction factor in the Reynolds number calculation but only up to a size $d_0 \approx 30\ \mu$m. Thereafter, neglecting the slip correction results in less than 0.5% error in V_∞.

The present results and selected previous results for terminal velocity are compared in Table 3. The three basic drag formulas given in Table 2 were first used to calculate accurate terminal velocities for the laboratory conditions of Gunn and Kinzer, and then a root mean square (rms) and maximum velocity deviation were determined for each author's method. Since the present method is a sixth-order fit to the basic formulas, the deviations are understandably small. Since the formulas

of Berry and Pranger (1974) are a high order fit to modern drag data, the deviations are also quite small. On the other hand, the formulas of Foote and du Toit (1969), Wobus *et al.* (1971) and Dingle and Lee (1972) are all based on the data of Gunn and Kinzer. The larger deviations of these methods are due in part to the inherent inaccuracies of the data of Gunn and Kinzer for drops with diameters $\lesssim 0.4$ mm (as seen in Fig. 2 for $N_{Re} \lesssim 40$).

Although the present formulation is similar to the original third-order fit of Davies for a rigid sphere in the range $2 \lesssim N_{Re} \lesssim 10\,000$, the lack of good data available to Davies, especially at lower Reynolds numbers, led him to a considerably less accurate formulation as evidenced by the velocity deviations in Table 3. The error is also seen in the plot of Davies formula in Fig. 2. Consequently, the present formulation should replace Davies drag formulation for the rigid sphere in the range of $0.01 \leqslant N_{Re} \leqslant 300$ and should also replace the formulas based on the data of Gunn and Kinzer for falling water drops within size range $20\ \mu\text{m} \lesssim d_0 \lesssim 1$ mm.

TABLE 3. Terminal velocity deviations from the basic drag formulas in the range $20\ \mu\text{m} \leqslant d_0 \leqslant 1$ mm at 20°C, 1 atm and 50% relative humidity.

Author(s)	rms deviation (%)	Maximum deviation (%)	Range*
Beard [Table 1]	0.09	0.6	$20\ \mu\text{m} \leqslant d_0 \leqslant 1$ mm (25 pts.)
Berry and Pranger [Their Eqs. (8) and (9)]	1.1	3.2	$20\ \mu\text{m} \leqslant d_0 \leqslant 1$ mm (25 pts.)
Gunn and Kinzer [experimental data]	3.3	8.0	$0.1 \leqslant d_0 \leqslant 1$ mm (10 pts.)
Foote and du Toit [Their Eq. (9), $N=9$]	3.5	13.7	$0.1 \leqslant d_0 \leqslant 1$ mm (23 pts.)
Dingle and Lee [Their Eq. (4a)]	3.6	8.0	$0.1 \leqslant d_0 \leqslant 1$ mm (10 pts.)
Wobus *et al.* [Their Eq. (4)]	3.3	8.0	$0.1 \leqslant d_0 \leqslant 1$ mm (10 pts.)
Davies [His Eq. (6)]	2.4	7.5	$0.1 \leqslant d_0 \leqslant 1$ mm (22 pts.)

* The number of points used in each range is shown in parentheses.

5. Raindrops ($1\ \text{mm} \lesssim d_0 \lesssim 7\ \text{mm}$)

a. General remarks on velocity fluctuations

Modern measurements of the terminal velocity of large water drops were carried out by Laws (1941), Davies [quoted by Sutton (1942) and Best (1950)], and Gunn and Kinzer (1949). These investigators observed quite similar velocities for corresponding drop sizes at sea level conditions. Considering the unsteady nature of the wake of a drop falling with $N_{Re} \gtrsim 300$, and considering the resonance mechanism suggested by Gunn (1949) in which the vibrational modes of a drop are excited by vortex shedding, one would expect that the drag on a drop and thus its fall velocity would fluctuate. However, the velocity response of the drop to any change in drag force is limited by the relaxation time which at these Reynolds numbers is of order $V_\infty/g \sim 1$ s. Since the frequency at which resonance occurs, for any vibration mode, is higher than 400 Hz, it seems reasonable to conclude that such rapid shape fluctuations would not result in any significant velocity changes. Indeed, no experimental evidence was reported on velocity fluctuations in the above studies of drops falling in still air.

Whereas drops falling at equilibrium in still air should maintain a steady velocity, drops falling in the atmosphere must constantly adjust to turbulence. In fact, the general relationship between the essential variables shown in (1) should be augmented to include the characteristics of the turbulence encountered by the raindrop. Evidence of the effect of turbulence on raindrop velocity is scant. Laws found about a 2% reduction in raindrop velocity for six rain cases when compared to his still air measurements. These results are not very conclusive due to large scatter, lack of data (only 24 raindrops measured), and the rather primitive method used for determining raindrop size. No information at all is given on the degree of turbulence.

The extent to which turbulence can affect the shape of raindrops has been documented by Jones (1959) from nearly 2000 photographs of raindrops at ground level. He found that the shape varied considerably for a given size from oblate to prolate spheroidal. For example, at $d_0 \approx 4$ mm the axis ratio ranged between 0.5 and 1.3 with a mean value of 0.85. The distribution of axis ratios was found to be skewed toward the higher axis ratios. Consequently, the mean axis ratios found by Jones are significantly larger than those measured in the laboratory or computed empirically for still air (Pruppacher and Pitter, 1971).

It is not clear how such large drop distortions may affect the velocity. A calculation of the time average velocity is beyond the present knowledge of the instantaneous forces on a raindrop falling in turbulent air. From the results of Jones, it is tempting to speculate that the time average drag coefficient is lower for turbulent air because the average shape is less oblate. However, the information available on raindrop velocities under natural conditions due to Laws indicates that the average drag coefficient may actually be higher in turbulent air.

Since sufficient experimental evidence is lacking to establish even a tentative relationship between the average raindrop velocity and the degree of turbulence, and since no velocity measurements with reliable independent size evaluations are available for raindrops falling under natural conditions, use will be made of the best available velocity measurements for still air. If the field observations of Laws are at all indicative of the effect of turbulence, then the velocity estimates based on still air measurements may be within a few percent of the fall velocities in the atmosphere.

b. Terminal velocity in still air

The effect of the reduced air density on the terminal velocity of raindrops must now be considered in order to derive a formulation for the terminal velocity of drops aloft. Measurements of the fallspeed of drops in still air for reduced air density have been carried out by Davies [quoted by Sutton (1942) and Best (1950)]. Unfortunately, Sutton has acknowledged that these data are probably in error for the larger drops due to an insufficient fall distance of 11 m. For sea level density Laws found that 20 m was needed for larger drops to reach ~99% of terminal velocity. However, even with a 20 m distance, the largest drop, $d_0 \approx 6.1$ mm, did not attain a consistent velocity probably because it had not achieved equilibrium shape. Gunn and Kinzer used a 20 m fall distance and reported no data for $d_0 > 5.8$ mm perhaps due to the same problem in establishing the equilibrium shape and velocity for very large drops.

In a comparison by Lane and Green (1956), the velocities for Davies for sea level conditions are seen to be a few percent lower than those of Laws and of Gunn and Kinzer. Although the errors in the Davies data are small at sea level, they increase considerably at reduced air densities because the distance needed for large raindrops to reach terminal velocity varies approximately with the inverse of the air density. Thus, the velocity scheme of Foot and du Toit (1969) derived from Davies data predicts velocities that are erroneously low. Unfortunately, there are no other measurements for water drops falling at reduced air densities available which could be used to update their empirical formula.

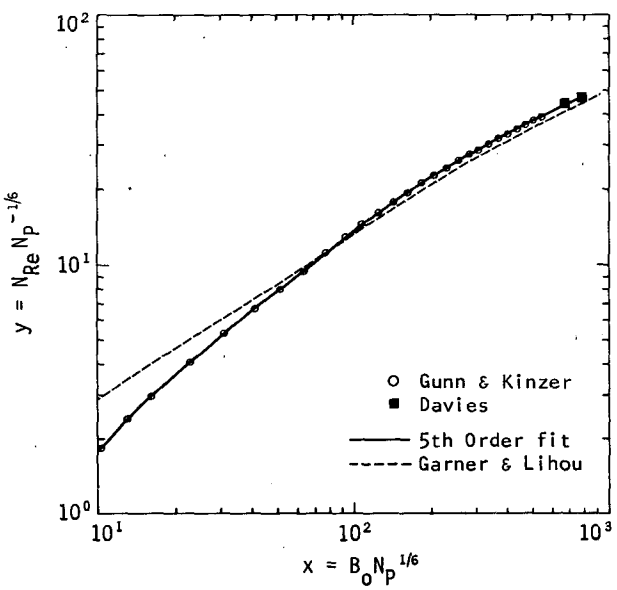

FIG. 3. Relation between the dimensionless group $x = \mathrm{Bo} N_P^{1/6}$ and $y = N_{Re} N_P^{-1/6}$ for liquid drops falling at terminal velocity in air.

c. Empirical correlation of physical property effects

Instead of awaiting new measurements, the complexity of the problem can be reduced by inspection. The remaining variables may then be used to form a set of dimensionless groups from which a relation for the terminal velocity may be derived using data existing in the literature. Since only the average vertical velocity is of interest, the time-dependent effects can be ignored while acknowledging that small velocity fluctuations may occur from wake instabilities and air turbulence. The effects of internal viscosity may be neglected based on the arguments and evidence presented on the previous section. Thus, the terminal velocity problem for large water drops has been simplified to that of a noncirculating water drop of equilibrium shape falling in still air. The relationship for the essential variables may now be written in the form

$$f(d_0, V_\infty, \rho, \eta, \sigma, D) = 0, \tag{13}$$

which reduces to only three independent dimensionless groups. The relation between three such independent groups was established experimentally by Garner and Lihou (1965) in a study on drops of various liquids supported by the airstream of a vertical wind tunnel (in terms of the Reynolds number N_{Re}, a modified Bond number $\mathrm{Bo} = 4N_{Bo}/3$, and a physical property number that is formed by eliminating the diameter from the Davies and Bond numbers, i.e., $N_P = 9N_{Da}^2/16N_{Bo}^3 = \sigma^3\rho^2/\eta^4\Delta\rho g$). Garner and Lihou found that a plot of logBo vs $\log N_P$ gave straight, parallel lines for each N_{Re} with a slope of -0.471. Similarly, they found straight, parallel lines for each N_P in a plot of logBo vs $\log N_{Re}$ with a slope of 1.83 for $N_{Re} \gtrsim 1500$. The final relation was obtained from $\mathrm{Bo} \propto N_{Re}^{1.83} N_P^{-0.471}$ to yield $\mathrm{Bo} N_P^{1/6} \propto (N_{Re} N_P^{-1/6})^{1.83}$. A plot of their data for $x = \mathrm{Bo} N_P^{1/6}$ and $y = N_{Re} N_P^{-1/6}$ showed a very close fit to the curve $x = 0.75\ y^{1.83}$. Another curve $x = 1.96\ y^{1.52}$, obtained in a similar manner, showed a very close fit to data for $N_{Re} \lesssim 1500$.

d. Improved correlation for water drops

The above relations are compared to the well known sea level data of Gunn and Kinzer in Fig. 3. Although the results of Garner and Lihou differ somewhat from the data of Gunn and Kinzer, perhaps due to less precision in the wind tunnel measurements, their correlation is valuable in predicting the variation of the terminal velocity of large drops with the physical properties of the system. Therefore, it was necessary to improve the results of Garner and Lihou at sea level by using the measurements of Gunn and Kinzer while retaining the essential form of the correlation. For this purpose, the data of Gunn and Kinzer were fitted by the least-square method in $x = \log_e(\mathrm{Bo} N_P^{1/6})$ and $y = \log_e(N_{Re} N_P^{-1/6})$ shown as the fifth-order curve in Fig. 3. Also included are two data points of Davies in order to

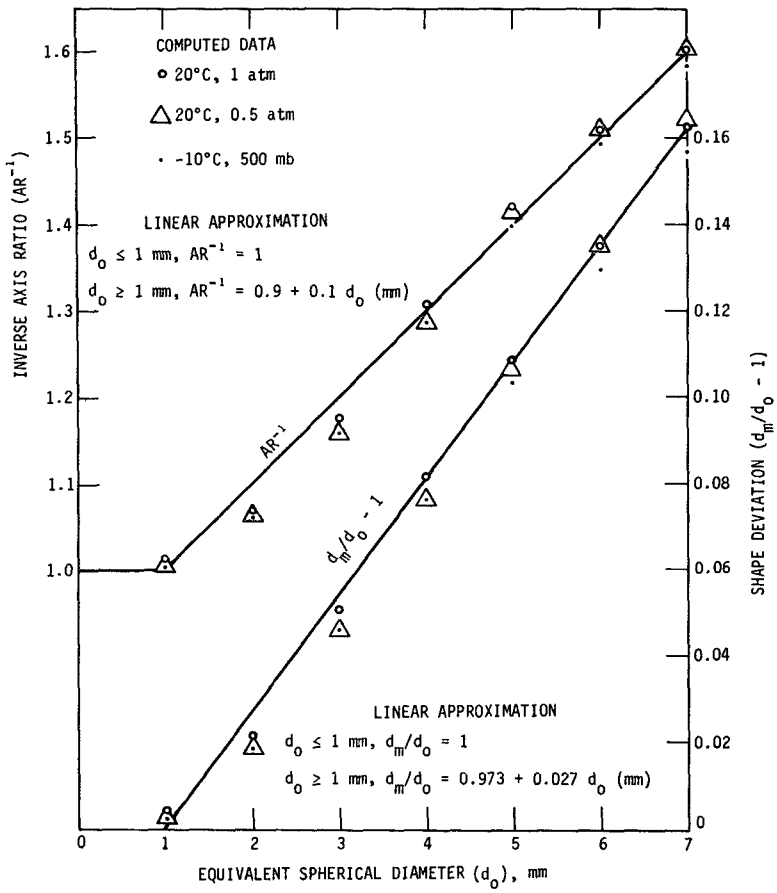

FIG. 4. Inverse axis ratio and shape deviation as a function of the equivalent spherical diameter for three combinations of temperature and pressure.

extend the velocity estimate to $d_0 = 7$ mm. The resulting formula in Table 1 (part 3) agrees within $\pm 0.5\%$ of the velocities of Gunn and Kinzer at sea level, and may be used for drops sizes 1.07 mm $\leqslant d_0 \leqslant$ 7 mm for an estimate of terminal velocities in the atmosphere for any reasonable atmospheric condition. The choice of $d_0 = 1.07$ mm as the transition size was determined by evaluating the formulas in adjacent ranges at three different conditions (20°C, 1.20 kg m^{-3}; 20°C, 0.60 kg m^{-3}; −10°C, 0.66 kg m^{-3}). These computations yielded crossover sizes within the range $d_0 = 1.07 \pm 0.01$ m.

e. Drop shape results

The terminal velocities derived by the present method were used to determine the drop shape as a function of d_0 and atmospheric conditions. Use was made of the semi-empirical formulation of Pruppacher and Pitter (1971) in which the shape is calculated from an evaluation of (10) by approximating the differential dynamic pressure by the aerodynamic pressure distribution about a sphere obtained empirically. The results are shown in Fig. 4 in terms of the inverse axis ratio and the shape deviation.

The inverse axis ratio is the ratio of the maximum or so-called projected diameter (d_m) to the height obtained from the drop's silhouette. The shape deviation is the deviation of the distortion factor (d_m/d_0) from unity and may be used to obtain d_m. Both shape parameters reveal only very slight changes in shape with changes in atmospheric conditions over the range from 1 atm at 20°C, to 500 mb at −10°C, and a hypothetical test case for 20°C at 0.5 atm.

Considering the approximate nature of both the velocity and shape calculations, it is doubtful that anything very significant should be attributed to these minor changes in shape. Consequently, the following linear approximations may be used which are independent of the atmospheric conditions:

$$AR^{-1} = 0.9 + 0.1 d_0[\text{mm}], \tag{14}$$

$$d_m/d_0 = 0.973 + 0.027 d_0[\text{mm}]. \tag{15}$$

This result is somewhat expected in the light of the finding of Green (1975) who has calculated the shape by considering only the hydrostatic terms in (10). It is quite evident from a comparison of the shape determined by Green with that computed by Pruppacher

and Pitter that the aerodynamic pressure serves to distort the pure oblate shape determined by hydrostatics alone. However, the axis ratio and projected diameter remain essentially unaffected, so that the primary spheroidal shape is a function only of the hydrostatic dimensionless group, $N_{Bo}=\Delta\rho g d_0^2/\sigma$. For a drop falling in the atmosphere the Boud number varies mainly with the raindrop size since an atmospheric change from 20°C to −10°C can only reduce N_{Bo} by a maximum of 6%.

f. Drag coefficient results

The relation between the present and previous results is best understood from an analysis of the drag coefficient shown in Fig. 5. It is especially helpful to consider the drag coefficient curve for a particular raindrop shape since the hydrostatic and dynamic methods have shown that drops falling in still air are essentially shape invariant with changing atmospheric conditions. Although no information exists for raindrop shapes that are more complex than oblate spheroids, use can be made of the fact that all spheroids have similar C_D curves as long as the flow is steady (Stringham *et al.*, 1969). This similarity is seen between curve 1 for the rigid sphere, based on the drag formulas in Table 2, and curve 2 for an oblate spheroid with AR=0.52 after Stringham *et al.* If C_D and N_{Re} were to be calculated using d_m instead of d_0, then the oblate spheroid curve would be somewhat closer to the sphere curve. However, the two curves remain quite distinct (Stringham *et al.*) because of the intrinsically different flow about an oblate spheroid compared to a sphere.

Since no reliable data are available for oblate spheroids with axis ratios which approximately correspond to the shape of large raindrops, the mean value of curves 1 and 2 was taken to represent an oblate spheroid with an intermediate axis ratio of AR≈0.76. The interception of curve 3 with the empirical findings of Gunn and Kinzer (curve 4) occurs at $d_0=4.5$ mm, a size that has an axis ratio of 0.73 according to the method of Pruppacher and Pitter.

The various methods for predicting the terminal velocity of a 4.5 mm drop at 20°C and a reduced air density of 0.60 kg m^{-3} can now be examined after calculating the drag coefficient from $C_D=4\Delta\rho g d_0/(3\rho V_\infty^2)$. The result of Foote and du Toit shows an increased drag coefficient which originates in the erroneously low terminal velocities of Davies. The values computed by Berry and Pranger lie on curve 4 since the drag coefficient curve of Gunn and Kinzer was used as the constraint for the velocity adjustment. Both of these results indicate a considerable change in shape. The drag coefficient result of the present method for the 4.5 mm drop at 0.60 kg m^{-3} is seen to lie very close to the estimated C_D curve for constant shape, which is quite consistent with the prior shape analysis. Thus, the present method for calculating V_∞ is independently verified by the near coincidence of the calculated value of C_D with the curve of constant shape.

The data points computed for lower air densities lie on the single dashed curve which is determined by the unique relation for C_D in terms of N_{Re} at constant Davies number (i.e., $C_D=N_{Da}N_{Re}^{-2}$). If the drag co-

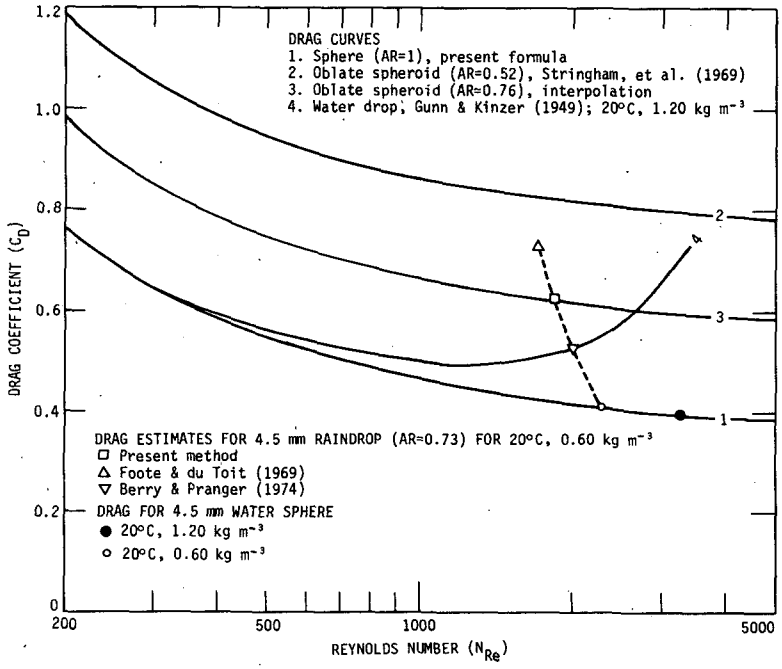

FIG. 5. Drag coefficient of a rigid sphere, oblate spheroids, and water drops falling at terminal velocity in air at sea level as a function of the Reynolds number.

efficient itself is assumed to be invariant with a change in air density, then the point for the 4.5 mm drop at 0.6 kg m^{-3} would lie on the dashed curve at $C_D=0.6$. A constant C_D estimate is only reasonable as long as the slope of the drag curve is small. As the drop size decreases, the use of a constant C_D becomes progressively worse because of the increased steepness of the appropriate C_D curve.

A method devised by Battan (1964) can also be evaluated using the C_D curves. For this method the sea level velocity for the drop is multiplied by the ratio of the velocities of an equivalent water sphere at a reduced air density to that at sea level. This method determines the adjusted drag coefficient by multiplying the sea level drag coefficient for the drop by the ratio of the drag coefficients for a water sphere at a reduced air density to that at sea level. The values of C_D for the 4.5 mm water sphere are shown in Fig. 5. The efficacy of Battan's method is due to the invariance of drop shape and the fact that all spheroid drag coefficient curves have similar characteristics. Thus, the method of Battan yields a drag coefficient correction based on the C_D curve for a sphere that is close to the actual C_D adjustment for a drop of constant shape.

g. Terminal velocity results

The present and previous results for the terminal velocity of raindrops are compared in Fig. 6. It is evident from curve 1 that the present method closely fits the data of Gunn and Kinzer whereas the data of Davies for the same air density of 1.20 kg m^{-3} are seen to lie somewhat below the curve. When the density is reduced to 0.60 kg m^{-3}, the velocity obtained by the present method is as much as 9% higher than that of Foote and du Toit and considerably lower than the formula of Berry and Pranger which supposedly extends to $d_0=5.8$ mm. This latter method assumes that the larger drops change shape aloft only along the drag coefficient curve of Gunn and Kinzer. There is no physical basis for this assumption; in fact, as Foote and du Toit have pointed out, such a restraint leads to an excessively large terminal velocity aloft. For the largest raindrop sizes, there is close agreement between the present result and the constant drag coefficient method given by curve 5 obtained from $\rho V_\infty^2=$ constant. This method provides a simple means of estimating V_∞ aloft although the error increases as the size decreases. For $d_0<1$ mm the constant C_D method is incompatible with the actual variation of C_D for a drop, i.e., C_D for the rigid sphere. In constrast, the method of Battan predicts fall velocities at a reduced air density that differ only slightly from the present result even for the smaller raindrops. This close agreement was expected on the basis of the drag coefficient analysis. However, the use of this alternative method requires the calculation of rigid sphere vaelocities and cannot be used readily unless a relationship between N_{Re} and N_{Da} is developed for the range $300\leqslant N_{Re}\leqslant 4000$. Therefore, the present result given in Table 1 (part 3) is more convenient because terminal velocities can be calculated directly from the raindrop size and atmospheric conditions.

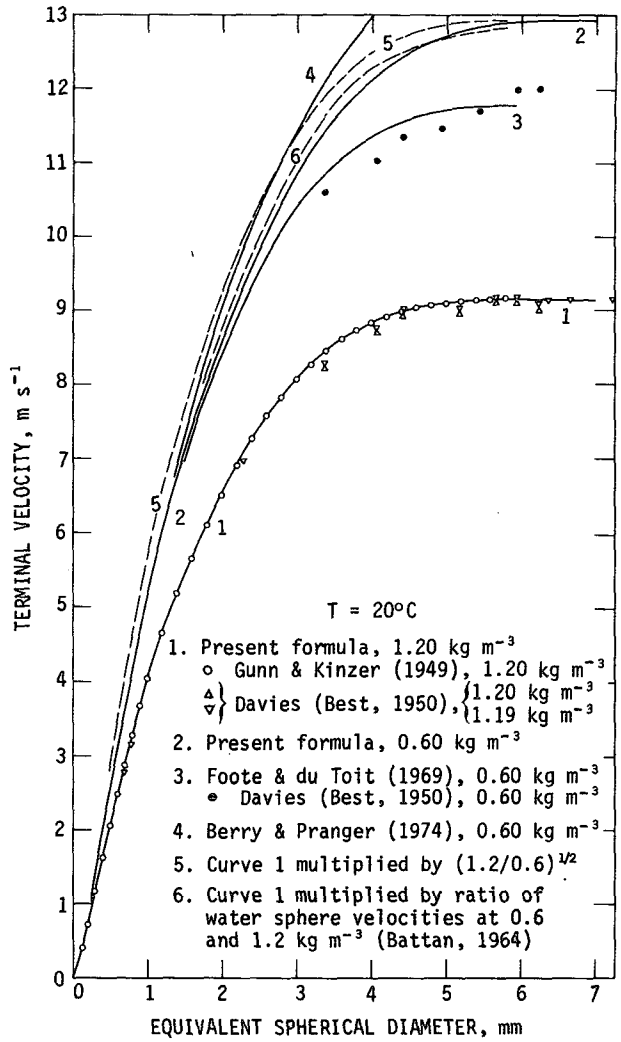

FIG. 6. Comparison of the terminal velocity of raindrops aloft based on various methods as a function of the equivalent spherical diameter. Also shown are the basic data and resulting curve for sea level.

For estimating raindrop velocities aloft by the present method, the summer-time atmosphere of Foote and du Toit was assumed in which the air density is reduced to a value of 0.66 kg m^{-3} at 500 mb. The terminal velocities for five levels are shown in Fig. 7 along with the sea level result of Gunn and Kinzer. The velocity for large raindrops is seen to increase considerably from a sea level value of 9 m s^{-1} to a 500 mb value in excess of 12 m s^{-1}.

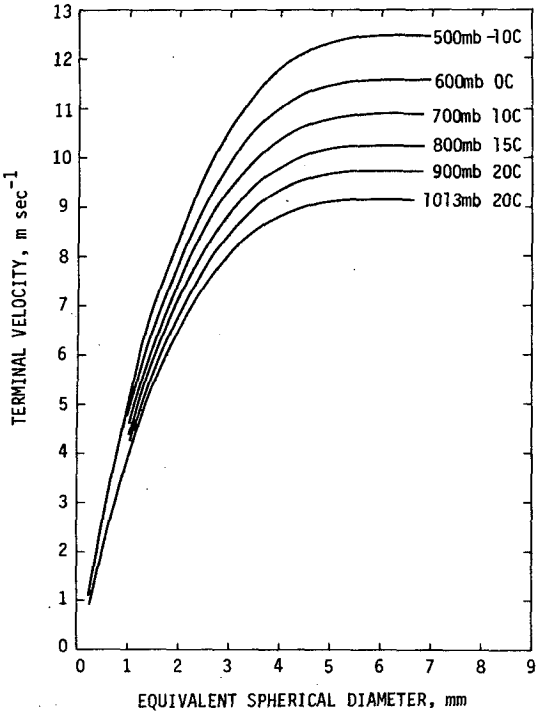

FIG. 7. Terminal velocity of raindrops at five pressure levels in a summer atmosphere as a function of the equivalent spherical diameter. Also shown in the standard curve for sea level.

6. Conclusions

Three semi-empirical formulas have been developed for the terminal velocity of water drops applicable to all atmospheric conditions which are based on three physically distinct flow regimes:

1) Slip flow about a rigid sphere at negligible Reynolds numbers ($10^{-6} \lesssim N_{Re} \lesssim 0.01$), $0.5\ \mu m \leqslant d_0 \leqslant 19\ \mu m$.

2) Continuum flow past a rigid sphere at low and intermediate Reynolds numbers ($0.01 \lesssim N_{Re} \lesssim 300$), $19\ \mu m \leqslant d_0 \leqslant 1.07$ mm.

3) Continuum flow around a non-circulating water drop of equilibrium shape at moderate to large Reynolds number ($300 \lesssim N_{Re} \lesssim 4000$), $1.07\ mm \leqslant d_0 \leqslant 7$ mm.

In the lower regime the effects of slip were accounted for by use of a first-order Knudsen number correction in the Stokes-Cunningham factor applied to a rigid sphere in Stokes flow. The variation of the mean free path with atmospheric conditions, obtained from kinetic theory, was found to differ from formulas presented in the literature.

In the flow regime for low to intermediate Reynolds numbers, the effects of a varying surface tension and internal viscosity were shown to have a negligible influence on the shape and terminal velocity of a falling drop for $d_0 \lesssim 1$ mm. Thus, the problem reduced to determining the terminal velocity for a rigid sphere. The final formula for V_∞ was developed after an analysis of the relevant theoretical and experimental data, and the result was found to differ somewhat from methods based on the data of Gunn and Kinzer, especially for smaller drops.

In the upper flow regime the effects of the unsteady wake did not appear to perturb the vertical velocity significantly. Although air turbulence was found to have a marked effect on raindrop shape, the values of V_∞ in the literature for natural rainfall differed only slightly from laboratory measurements. Because no quantitative information existed on the relation between raindrop velocity and turbulence, the problem was centered on obtaining estimates of the terminal velocity for drops falling in still air, which reduced to finding the relation between the three dimensionless groups for the terminal velocity of a noncirculating water drop of equilibrium shape in still air. The results of Garner and Lihou for drops of various liquids suspended in the airstream of a wind tunnel provided the relation for the variation of V_∞ with the physical properties. The data of Gunn and Kinzer were then used to obtain the final formula for V_∞. An analysis of the drop shape resulting from use of the present velocities in the scheme of Pruppacher and Pitter revealed that the shape was essentially invariant with atmospheric conditions. This conclusion was consistent with the subsequent analysis of the drag coefficient that demonstrated how the present value of C_D varied for different atmospheric conditions along a curve of constant shape. Two simple formulas were given for the axis ratio and the projected diameter both as a function of only the drop size d_0. A comparison of the present result at a reduced air density with the previous methods for calculating V_∞ aloft showed that the scheme of Foote and du Toit predicted velocities that were too small, whereas the method of Berry and Pranger predicted velocities that were too large. On the other hand, the method of Battan proved to be in close agreement with the present result over the entire range of raindrop sizes.

The formulas for all three ranges were tested at the crossover points and found to merge smoothly even at an extreme condition of 500 mb and -10°C. The given formulas can be utilized in a computer program by specifying the physical properties $(T,p,\rho.\Delta\rho,\eta,\sigma,g)$ in order to obtain V_∞, d_m and AR directly from d_0, or obtain d_0, d_m and AR from V_∞ by simple iteration.

Acknowledgments. The author is in debt to H. R. Pruppacher whose research on the drag and shape of falling drops has greatly contributed to this result. The author also appreciates the helpful discussions of G. B. Foote of the National Center for Atmospheric Research, H. R. Pruppacher of the University of California at Los Angeles, and H. T. Ochs, R. Cataneo and R. G. Semonin of the Illinois State Water Survey. This research would not have been possible without the financial support of the National Science Foundation (GA-32814X), the Environmental Protection Agency

(R-802183), and the Energy Research and Development Agency (ERDA-1199).

APPENDIX

List of Symbols

AR	axis ratio
Bo	modified Bond number [$=4N_{Bo}/3$]
c, c'	proportionality constants for Knudsen number correction to Stokes drag
C_D	drag coefficient [$\equiv 8D(\pi d_0^2\rho V_\infty^2)^{-1} = 4\Delta\rho g d_0/(3\rho V_\infty^2)$]
C_{sc}	slip correction factor
D	drag force at terminal velocity [$=\pi d_0^3\Delta\rho g/6$]
d_0	equivalent spherical diameter
d_m	maximum diameter (i.e., projected diameter)
g	acceleration of gravity [$\equiv 9.8$ m s^{-2}]
i	subscript for inner fluid (i.e., water)
l	mean free path of air molecules
N_{Bo}	Bond number [$\equiv\Delta\rho g d_0^2/\sigma$]
N_{Da}	Davies number [$\equiv C_D N_{Re}^2 = 4\rho\Delta\rho g d_0^3/3\eta^2$]
N_{Kn}	Knudsen number [$\equiv l/d_0$]
N_P	physical property number [$\equiv\sigma^3\rho^2/\eta^4\Delta\rho g$]
N_{Re}	Reynolds number [$\equiv\rho V_\infty d_0/\eta$]
N_{Sr}	Strouhal number [vortex shedding frequency times d_0/V_∞]
0	subscript for standard condition (1 atm, 20°C)
$\mathcal{P}$	total fluid pressure (i.e., static plus dynamic)
p'	dynamic pressure
p	static pressure
R_1, R_2	principal radii of curvature
s	subscript for Stokes solution
T	thermodynamic temperature
t	time
V	fluid velocity
V_∞	terminal velocity
X	$\log_e(N_{Re})$ or $\log_e(x)$
x	$\text{Bo}N_P^{1/6}$
Y	$\log_e(N_{Da})$ or $\log_e(y)$
y	$N_{Re}N_P^{-1/6}$
Δ	difference between fluid properties of drop and air (e.g., $\Delta\rho=\rho_i-\rho$)
η	dynamic viscosity
ρ	fluid density
σ	surface tension

REFERENCES

Abraham, F. F., 1970: Functional dependence of drag coefficient of a sphere on Reynolds number. *Phys. Fluids*, **13**, 2194–2195.

Achenbach, E., 1974: Vortex shedding from spheres. *J. Fluid Mech.*, **62**, 209–221.

Basset, A. B., 1961: *A Treatise on Hydrodynamics*, Vol. 2. Dover [referred to in Happle and Brenner, p. 125, see below].

Battan, L. J., 1964: Some observations of vertical velocities and precipitation sizes in a thunderstorm. *J. Appl. Meteor.*, **3**, 415–420.

Beard, K. V., and H. R. Pruppacher, 1969: A determination of the terminal velocity and drag of small water drops by means of a wind tunnel. *J. Atmos. Sci.*, **26**, 1066–1072.

Berry, E. X, and M. R. Pranger, 1974: Equations for calculating the terminal velocities of water drops. *J. Atmos. Sci.*, **31**, 108–113.

Best, A. C., 1950: Empirical formulae for the terminal velocity of water drops falling through the atmosphere. *Quart. J. Roy. Meteor. Soc.*, **76**, 302–311.

Chapman, S., and T. G. Cowling, 1970: *The Mathematical Theory of Non-uniform Gases*. Cambridge University Press, 423 pp.

Davies, C. N., 1945: Definitive equations for the fluid resistance of spheres. *Proc. Phys. Soc. London*, **A57**, 259–270.

Dingle, A. N., and Y. Lee, 1972: Terminal fallspeeds of raindrops. *J. Appl. Meteor.*, **11**, 877–879.

Epstein, P. S., 1924: On the resistance experienced by spheres in their motion through gas. *Phys. Rev.*, **23**, 710–733.

Foote, G. B., and P. S. du Toit, 1969: Terminal velocities of raindrops aloft. *J. Appl. Meteor.*, **8**, 249–253.

Garner, F. H., and D. A. Lihou, 1965: Mass transfer to and from drops in gaseous streams. *DECHEMA Monogr.*, **55**, 155–178.

Green, A. W., 1975: An approximation for the shapes of large raindrops. *J. Appl. Meteor.*, **14**, 1578–1583.

Gunn, R., 1949: Mechanical resonance in freely falling raindrops. *J. Geophys. Res.*, **54**, 383–385.

——, and G. D. Kinzer, 1949: The terminal velocity of fall for water drops in stagnant air. *J. Meteor.*, **6**, 243–248.

Hadamard, J., 1911: Mouvement permanent lent d'une sphere liquid et visqueuse dans un liquid visqueux. *Compt. Rend.*, **152**, 1735–1738.

Happel, J., and H. Brenner, 1965: *Low Reynolds Number Hydrodynamics*. Prentice-Hall, 553 pp.

Jones, D. M., 1959: The shape of raindrops. *J. Meteor.*, **16**, 504–510.

Knudsen, M., and S. Weber, 1911: Resistance to motion of small spheres. *Ann. Phys.*, **36**, 981–994.

Lane, W. R., and H. L. Green, 1956: *Surveys in Mechanics*, G. T. Batchelor, Ed. Cambridge University Press, 475 pp.

Laws, J. O., 1941: Measurements of the fall velocity of water drops and rain drops. *Trans. Amer. Geophys. Union*, **22**, 709–721.

LeClair, B. A., A. E. Hamielec and H. R. Pruppacher, 1970: A numerical study of the drag on a sphere at low and intermediate Reynolds numbers. *J. Atmos. Sci.*, **27**, 308–315.

——, A. E. Hamielec, H. R. Pruppacher and W. D. Hall, 1972: A theoretical and experimental study of the internal circulation in water drops falling at terminal velocity in air. *J. Atmos. Sci.*, **29**, 728–720.

Magarvey, R. H., and C. S. MacLatchy, 1965: Vortices in sphere wakes. *Can. J. Phys.*, **43**, 1649–1656.

Maxworthy, T., 1965: Accurate measurements of sphere drag at low Reynolds numbers. *J. Fluid Mech.*, **23**, 369–372.

Möller, W., 1938: Experimentelle Untersuchungen zur Hydrodynamik der Kugel. *Phys. Z.*, **39**, 57–80.

Perry, J., 1950: *Chemical Engineering Handbook*. 3rd ed. McGraw-Hill, 1017 pp.

Perry, R. H., and C. H. Chilton, 1973: *Chemical Engineering Handbook*, 5th ed. McGraw-Hill, 1958 pp.

Proudman, I., and J. R. A. Pearson, 1957: Expansions at small Reynolds numbers for the flow past a sphere and a circular cylinder. *J. Fluid Mech.*, **2**, 237–262.

Pruppacher, H. R., and K. V. Beard, 1970: A wind tunnel investigation of the internal circulation and shape of water drops falling at terminal velocity in air. *Quart. J. Roy. Meteor. Soc.*, **96**, 247–256.

——, LeClair, B. P., and A. E. Hamielec, 1970: Some relations between the drag and flow pattern of viscous flow past a sphere and a cylinder at low and intermediate Reynolds numbers. *J. Fluid Mech.*, **44**, 781–790.

——, and R. Pitter, 1971: A semi-empirical determination of the shape of cloud and rain drops. *J. Atmos. Sci.*, **28**, 86–94.

Rybczynski, W., 1911: *Bull. Acad. Caracovie*, Ser A., p. 40 [referred to in Happle and Brenner, p. 127, see above].

Stringham, G. E., D. B. Simons and H. P. Guy, 1969: The behavior of large particles falling in quiescent liquids. *Geol. Sur. Prof. Pap.*, No. 562-C, 36 pp.

Sutton, O. G., 1942: Investigations on falling drops carried out at the Chemical Defense Experimental Station, Porton. *Meteor. Res. Pap.*, No. 40, 9 pp.

Taneda, S., 1956: Experimental investigation of the wakes behind cylinders and plates at low Reynolds numbers. *J. Phys. Soc. Japan*, **11**, 302–307.

Taylor, T. D., and A. Acrivos, 1964: The deformation and drag on a falling viscous drop at low Reynolds numbers. *J. Fluid Mech.*, **18**, 446–470.

Wobus, H. B., F. W. Murray and L. R. Koenig, 1971: Calculation of the terminal velocity of water drops. *J. Appl. Meteor.*, **10**, 751–754.